Role of carboxylic acid on the conductance behaviour of polyaniline

A. Ananda Jebakumar
Department of Chemistry, Government Polytechnic College for Women, Madurai, Tamilnadu, India-625011

Abstract

Conducting polymer-based composites have recently become popular in both academic research and industrial practices. The conductance mechanism of conductance can be accomplished through its interaction with other compounds and this can be fulfilled through compositing. Here composites of PANI and amino acids are reported through computation along with physical and chemical studies. PANI composites of (*E*)-3-phenylprop-2-enoic acid (CIA) and 3-hydroxy benzoic acid (3HBZA) are used to calibrate the factors of conductance in PANI. Conductance of PANI-CIA is higher than PANI-3HBZA due to electronic effect. The conductance is due to the quantum hoping of H^+ by the field produced by the polymer chain and the counter ion.

1. Introduction

Conducting polymers can be referred to as the chemical composite materials comprising polymeric components and conductive components [1]. Compositing is essential for day to day life besides scientific interest [2]. Energy harvesting, transport and storage are the need of the hour [3], in which conducting polymers have a significant role [4]. Between the conducting polymers, polyaniline (PANI) is well known for its varied applications and simplicity in preparation [5]. The emeraldine salt form of polyaniline is mentioned here as PANI in which the emeraldine base is the polymeric component and hydrogen chloride is the conductive part [6]. Compositing with discrete molecules can be of academic attention to get insight into the behaviour of polymers [7]. Further discrete covalent molecules as additive for composites are more significant to get physico-chemical aspects of charge mobility on organic metal, the conducting polymers, which elevates to the status of conductor from the insulator by slight modification in their composition using small molecular addition [8]. Computational study is a back bone of research by providing reasonable results and factors to understand the scientific phenomenon behind a research [9]. In this sense DFT is a worthwhile study [10] and blending computation along with experimental gives a good result [11]. As PANI is obtained from the addition of inorganic acid HCl, estimation of the role of organic acid on the conductance of PANI becomes noteworthy [12]. To accomplish this

ideology this study concentrates on the PANI composites of organic carboxylic acids. Here two carboxylic acids (CA) are chosen one is unsaturated acid (*E*)-3-phenylprop-2-enoic acid (CIA) and another is 3-hydroxy benzoic acid (3HBZA), a hydroxyl acid through DFT, synthesis, spectral and conductance studies along with statistical analysis.

2. Experimental

2.1 Synthesis of Composites

All the chemicals used were of AR grade obtained from Merk, India and used as such. PANI is synthesised by method elsewhere [13]. Slurry was prepared by 400 mg of PANI and 100 mg of CIA in 4 ml of DMSO using mortar and pestle. The content was dried at 70 °C for 24 hrs. Weight loss method was employed to check the complete removal of DMSO from the mixture. The composite was powdered and stored in a polyethylene container. The same procedure was repeated with 200, 300 and 400 mg of CIA and 3HBZA.

2.2 Computation

DFT studies were performed by B3LYP/ 6-31G** basis set in gas phase at 25 °C using firefly software [14] in i7 computer. TDDFT calculations were done using ORCA programme [15] by B3LYP/PBE0. Due to higher computational cost, the modeling studies were carried for each one unit of phenyl and phenylene rings for PANI, its composites and data related to PANI are reported somewhere else [16].

2.3 Equipment

DC conductance was recorded in Four Probe SES-Model DFP-RM. IR spectra were recorded in JASCO FT/IR-4600, UV-VIS in JASCO V-650 (DMSO) and luminescence in Perkin Elmer, LS 45, excitation at 380 nm (DMSO).

2.4 Analysis

Regression analysis was carried out for conductance studies. The equations used were; for ideal-$y = y_0+ax$; for real- $y = y_0+ax+bx^2$. The ideal behaviour means the expected trend of conductance.

3. Results and discussion

The role of AA on the DC conductance of PANI is studied based on the structural as well as electronic aspects. The structural components also known as steric effect is especially evaluated through geometrical parameters while the role of electronic effects by charge distribution likes atomic charge density, dipole moment and so on. Influence of AA on PANI is the perturbation of the above two effects.

3.1 Stability and Structure

The structure and stability details are given in Fig. 1 and structural data are given in Table 1. PANI-CIA has slightly higher stability over PANI-3HBZA. This slight enhancement may be due to the presence of unsaturation in the former. The $H_{1'}$-$Cl_{2'}$ and N_1-$H_{1'}$ bond lengths suggest that the $H_{1'}$ atom binds the N_1 strongly in PANI-3HBZA over its counterpart with an average strength ratio of 8:1 with respect to PANI. There is no significant difference in the other bond lengths, bond and dihedral angles for PANI-CIA and PANI-3HBZA from PANI. The approach angle of $H_{1'}$-$Cl_{2'}$ in PANI-CIA is comparable with PANI, while PANI-3HBZA has an ~ 11° increase. Hence, the steric effect is higher in the case of PANI-3HBZA over PANI-CIA. Due to the enhanced electronic and less steric effects, the conductance of PANI-CIA is higher than PANI-3HBZA.

3.2 Charge Density

Table 2 has the values of charge density. The charge density on $H_{1'}$ and $Cl_{2'}$ of PANI-3HBZA is increased by 34.3 and 74.2% respectively over PANI. In the case of PANI-CIA delocalisation of charges take place with a magnitude of 6.3 and 11.1 percentage respectively for $H_{1'}$ and $Cl_{2'}$ when compared to PANI. In general, the charge density of PANI-CIA is comparable with PANI. For H_{15} the charge density is 21.7 and 5.6 % higher for PANI-3HBZA and PANI-CIA than PANI. Thus, PANI-3HBZA has approximately three times more charge localisation over PANI-CIA. This higher delocalisation effect in PANI-CIA over PANI-3HBZA is due to the presence of a double bond in the CIA [17]. The above effect enhances the higher conductance of PANI-CIA over PANI-3HBZA. Even though the charges on $H_{1'}$ and $Cl_{2'}$ are increased for PANI-3HBZA over PANI and PANI-CIA, the drift velocity of the charge carriers in the quantum field produced between polymer and $Cl_{2'}$ is decreased in PANI-3HBZA. This adverse effect can be accounted for the loss of extended conjugation in PANI-3HBZA over others.

3.3 Dipole moment

Dipole moment values are given in Table 3. The percentage increase in the total dipole moment over PANI is 76 and 26% respectively for PANI-CIA and PANI-3HBZA. For PANI-3HBZA, the dipole moment along the *z*-axis is very low and for other axis the values are comparable with PANI-CIA. The dipole moment infers that conductance of PANI-CIA is higher than PANI-3HBZA with the charge mobility along the *z*-direction.

3.4 Molecular Orbitals

The MO diagrams are given in Fig.2. There is no much difference between the MOs of PANI-CA and the individual compounds. This may be due to the presence of benzene moiety in the PANI and CA. The major contribution for the HOMO and LUMO (Fig.3) are the benzene rings from PANI-CIA and PANI-3HBZA. The LUMO of PANI-CA is like PANI, while the HOMO of PANI-CIA is at CIA part and PANI-3HBZA on the PANI.

3.5 TDDFT

Table 4 has TDDFT values. The order of optical band gap based conductance is PANI-CIA > PANI-3HBZA and the order matches with the conductance. PANI-3HBZA has a blue shift while PANI-CIA has redshift with respect to PANI. Symmetry of PANI-3HBZAis distorted from PANI and PANI-CIA and has low conductance in PANI-3HBZA [18]. For PANI-3HBZA the transition at 366.9 nm is the combination of PANI→PANI and charge transfer transitions from the benzene ring of 3HBZA→EB. This infers that both charge transfer band and internal transition of EB are merged due to comparable energies. Among these two transitions, PANI→PANI predominates over the later. Behaviour of PANI-CIA differs from PANI and PANI-3HBZA. For PANI-CIA all the transitions are in the PANI part.

3.6 Frontier Molecular Orbital

The values of the above parameters are given in Table 5. The bandgap order of stability is PANI > PANI-CIA-16.7 %) > PANI-3HBZA (-41.7%) with respect to PANI and a negative sign indicates the low value. Based on the FMO parameters the order of conductance is PANI-3HBZA > PANI-CIA, which is the reverse of experimental. The higher conductance of PANI-CIA over PANI-3HBZA is accounted by the loss of symmetry in the later. Hence, it has been concluded that in addition to steric and electronic effects, symmetry also determines the property.

3.7 Polarizability

Table 6 has the values of polarizability. Polarizability of the PANI-CA is higher than CAs. There is a drastic increase in the value of γ over α and β. The order of the self-focusing effect is PANI-CIA>PANI-3HBZAwhichmatches with the order of conductance.

3.8 Spectra

IR has red and UV-VIS has blue shifts. The optical band gap of PANI-CIA is marginally lower than PANI-3HBZA and accounts for the conductance through polaron. Loss of symmetry in PANI-3HBZA may cause localisation of electrons. Fluorescence spectrum has a weak band at about 790 nm. This less intense emission explains the loss of electron

donor-acceptor pair. Fluorescence spectra of PANI-CA are less intense than PANI. Photoluminescence bands of PANI-CA are found in the violet and red regions.

3.9 Conductance

The conductance values are given in Table 7. PANI-CIA and PANI-3HBZA have a similar trend. PANI-CIA curve touches the ideal graph at the mole fraction of PANI 0.72. Coefficient 'a' is approximately 8 times less for PANI-CIA than PANI-3HBZA and 'b' is 5 times less. In general, the conductance of PANI-CIA is two times higher than PANI-3HBZA. The maximum deviation from the ideal behaviour is observed at the mole fraction of PANI for PANI-3HBZA at 0.5813 and 0.2371 for PANI-CIA. The difference in the conductance of compounds of 3.2.9 and this section is due to different compounds.

4. Conclusion

Charge mobility in PANI is evaluated through composites of PANI-CIA and PANI-3HBZA. The conductance of PANI-CIA is higher than PANI-3HBZA due to unsaturation in the later electronic effect. The mobility of charge in PANI is due quantum field hoping of proton between the polymer chain and the counter ion chloride.

5. References

1. G. Inzelt, Springer Science & Business Media, 2012.
2. Talita Greyling & Fiona Tregenna , Social Indicators Research, 2017,1 31, 887–930.
3. M.E. Kiziroglou, E.M. Yeatman, Materials and techniques for energy harvesting in Functional Materials for Sustainable Energy Applications, 2012
4. Aimee M. Bryan, Luciano M. Santino, Yang Lu, Shinjita Acharya, and Julio M. D'Arcy, Chem. Mater. 2016, 28, 17, 5989–5998.
5. Mama El Rhazi, Sanaa Majid, Miloud Elbasri, Fatima Ezzahra Salih, Larbi Oularbi & Khalid Lafdi, International Nano Letters, 2018, 8, 79–99.
6. Rajender Boddula and Palaniappan Srinivasan, Journal of Catalysts Volume 2014, 515428, 6
7. Shaoyun Fu, Zheng Sun, Pei Huang, Yuanqing Li, Ning Hu, Nano Materials Science, 2019,1, 2-30 .
8. Gagan Kaur, Raju Adhikari, Peter Cass, Mark Bown and Pathiraja Gunatillake, RSC Adv., 2015,5, 37553-37567
9. 9. K. Alzoubi, X.-Y. Li, Y. Wang, P.-J. Wan, and O. Frieder, IEEE Transactions on Parallel and Distributed Systems, 2003, 14, 4, 408–421.

10. Giuseppe Felice Mangiatordi, Eric Brémond, and Carlo Adamo, J. Chem. Theory Comput. 2012, 8, 9, 3082–3088
11. Theresa Sperger, Italo A. Sanhueza, and Franziska Schoenebeck, Acc. Chem. Res. 2016, 49, 6, 1311–1319
12. M. Yahia Abed Mona, Ali Youssif Hilda, A.Aziz M.A.Shenashen, Egyptian Journal of Petroleum, 2014, 23, 3, Pages 271-277.
13. Nazish Parveen, Mohammad Omaish Ansari, Thi Hiep Han & Moo Hwan Cho , Journal of Solid State Electrochemistry, 2017, 21, 57–68.
14. Granovsky, AA Baldridge, KK Boatz, JA Elbert, ST Gordon, MS Jensen, JH Koseki, S Matsunaga, N Nguyen, KA Su, S Windus, TL Dupuis, M & Montgomery, JA Journal of computational chemistry, 1993, 14, 11, 1347-136
15. Neese, F 2012, 'The ORCA program system', WIREs Computational Molecular Science, vol. 2, no. 1, pp. 73-78.
16. Gordana Ćirić-Marjanović, Maja Milojević-Rakić, Aleksandra Janošević-Ležaić, Sandra Luginbühl & Peter Walde, Chemical Papers, 2017, 71, 199–242.
17. Blythe, AR & Bloor, D (eds.) 2005, Electrical properties of polymers, Cambridge University Press, New York.
18. Pontes, RB Silva, EZD Fazzio, A & Silva, AJRD The Journal of the American Chemical Society, 2008, 130, 30, 9897-9903.

Figure 1 : Structure and Thermodynamic Stability

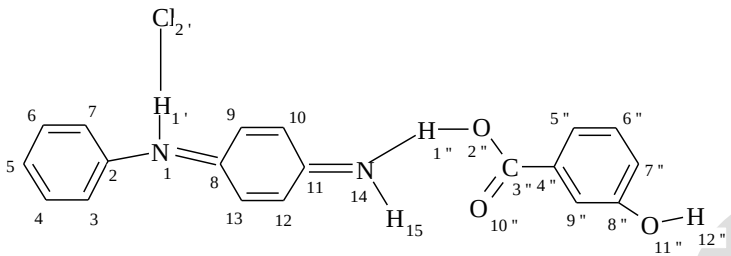

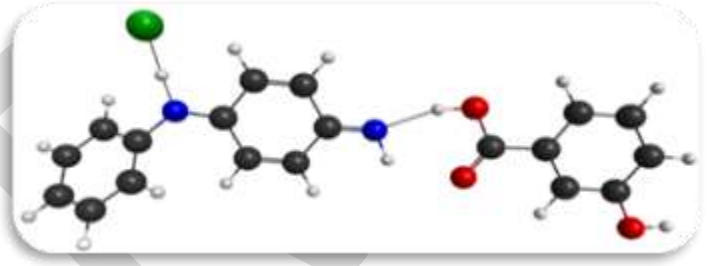

ES-3HBZA

(ES-3HBZA- (ES+3HBZA) = -45.6311 kJ/mole)

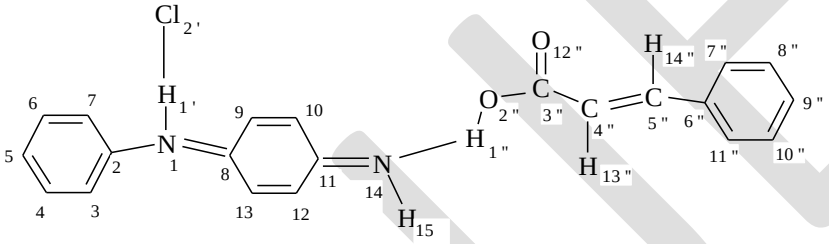

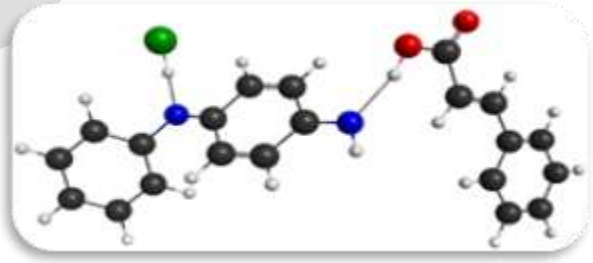

ES-CIA

(ES-CIA- (ES+CIA) = -45.7362 kJ/mole)

C-Black; H-White; O- Red; N-Blue; Cl-Green; S-Yellow

Figure 2 : MO Diagram

Figure3: MO Number, Name, Energy(eV) and AO Contribution to MO

3HBZA

36-HOMO (-6.286)
$C_{5''}$-1p_z; $O_{11''}$-1p_z

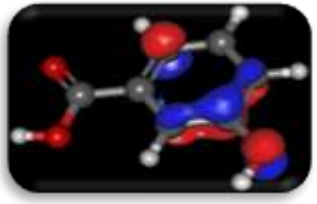

37-LUMO (-1.137)
$C_{7''}$-1p_z; $C_{3''}$-1p_z

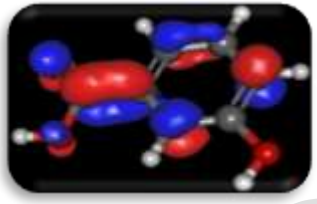

CIA

39-HOMO (-6.610)
$C_{4''}$-1p_z; $C_{4''}$-2p_z

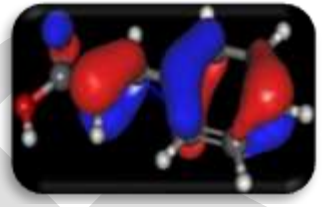

40-LUMO (-1.766)
$C_{5''}$-1p_z; $C_{5''}$-2p_z

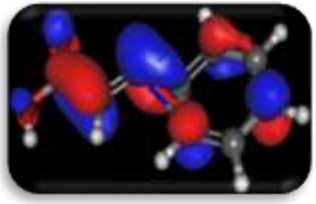

ES-3HBZA

88 HOMO-5 (-7.197)
C_2-1p_z; C_5-1p_z

89-HOMO-4 (-7.072)
$C_{4''}$-1p_z; $C_{7''}$-1p_z

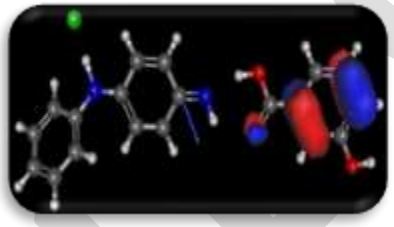

93-HOMO (-6.133)
$Cl_{2'}$-2p_z; $Cl_{2'}$-3p_z

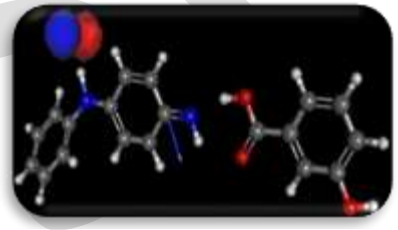

94-LUMO (-4.000)
N_{14}-1p_z; N_1-1p_z

ES-CIA

86 HOMO-10 (-8.441)
N_{14}-1p_y; N_{14}-1p_x

88 (-8.321)
$Cl_{2'}$-2p_x; $Cl_{2'}$-3p_x

95-HOMO-1 (-6.746)
C_5-1p_z; C_2-1p_z

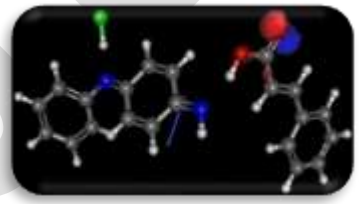

96-HOMO (-6.329)
$C_{4''}$-1p_z; $C_{4''}$-2p_z

97-LUMO (-3.317)
N_1-1p_z; N_{14}-1p_z

List of Tables

Table 1: Structural Parameters

Atom Pair	Bond Length (Å)		Atom Pair	Bond Angle (˚)		Atom Pair	Dihedral Angle(˚)	
	PANI-3HBZA	PANI-CIA		PANI-3HBZA	PANI-CIA		PANI-3HBZA	PANI-CIA
$H_{1'}$-$Cl_{2'}$	1.6589	1.3497	$Cl_{2'}$-$H_{1'}$-N_1	175.47	177.76	$Cl_{2'}$-$H_{1'}$-N_1-C_2	-93.46	82.38
N_1-$H_{1'}$	1.1903	1.7087	$H_{1'}$-N_1-C_2	114.54	114.32	$H_{1'}$-N_1-C_2-C_7	30.32	-38.74
N_1-C_2	1.4078	1.4030	$H_{1'}$-N_1-C_8	116.77	120.67	$H_{1'}$-N_1-C_8-C_9	12.27	-9.79
N_1-C_8	1.3117	1.3030	N_1-C_2-C_7	116.83	117.53	N_1-C_2-C_7-C_6	-178.34	177.84
C_2-C_3	1.4061	1.4083	C_2-C_3-C_4	119.55	120.00	N_1-C_8-C_{13}-C_{12}	-177.93	179.84
C_2-C_7	1.4061	1.4073	C_3-C_4-C_5	120.36	120.39	C_2-N_1-C_8-C_{13}	8.56	-9.62
C_3-C_4	1.3920	1.3929	C_5-C_6-C_7	120.47	120.39	C_2-C_3-C_4-C_5	-0.37	0.28
C_4-C_5	1.3971	1.3961	C_6-C_7-C_2	119.47	120.06	C_3-C_2-C_7-C_6	-3.03	3.12
C_5-C_6	1.3973	1.3979	C_7-C_2-C_3	120.16	119.33	C_4-C_3-C_2-C_7	2.52	-1.90
C_6-C_7	1.3911	1.3908	C_8-N_1-C_2	128.49	124.97	C_5-C_6-C_7-C_2	1.39	-2.16
C_8-C_{13}	1.4597	1.4680	C_9-C_{10}-C_{11}	121.67	121.17	C_8-C_{13}-C_{12}-C_{11}	0.00	0.00
C_9-C_{10}	1.3480	1.3475	C_{10}-C_{11}-C_{12}	116.93	117.03	C_9-C_{10}-C_{11}-C_{12}	1.86	-1.31
C_{10}-C_{11}	1.4652	1.4653	C_{11}-C_{12}-C_{13}	121.71	121.82	C_{10}-C_{11}-C_{12}-C_{13}	-2.91	2.75
C_{11}-C_{12}	1.4701	1.4683	C_{12}-C_{13}-C_8	120.36	120.91	C_{11}-N_{14}-H_{15}-$H_{1''}$	-180.00	-173.90
C_{11}-N_{14}	1.2887	1.2948	C_{13}-C_8-N_1	124.26	125.21	C_{12}-C_{11}-N_{14}-H_{15}	-0.93	0.00
C_{12}-C_{13}	1.3485	1.3477	N_{14}-C_{11}-C_{12}	123.54	123.91	C_{13}-C_{12}-C_{11}-N_{14}	178.53	-178.59
N_{14}-H_{15}	1.0272	1.0229						
N_{14}-$H_{1''}$	1.8242	1.8491						

Table 2 : Mulliken's Atomic Charge Density

PANI-3HBZA		PANI-CIA	
Atom	**Charge**	**Atom**	**Charge**
$H_{1'}$	0.2511	$H_{1'}$	0.1753
$Cl_{2'}$	-0.5666	$Cl_{2'}$	-0.2890
N_1	-0.6010	N_1	-0.5989
C_2	0.2563	C_2	0.2481
C_3	-0.0954	C_3	-0.0978
C_4	-0.0981	C_4	-0.0958
C_5	-0.0711	C_5	-0.0760
C_6	-0.0935	C_6	-0.0918
C_7	-0.0892	C_7	-0.0913
C_8	0.3498	C_8	0.3305
C_9	-0.1064	C_9	-0.0999
C_{10}	-0.0626	C_{10}	-0.0903
C_{11}	0.3119	C_{11}	0.3264
C_{12}	-0.1003	C_{12}	-0.1076
C_{13}	-0.0912	C_{13}	-0.0896
N_{14}	-0.6017	N_{14}	-0.6143
H_{15}	0.2823	H_{15}	0.2448

Table 3 : Dipole moment (D)

	μ_x	μ_y	μ_z	μ_{Total}
3HBZA	-0.8066	-1.9139	0.0000	2.0769
PANI-3HBZA	3.5846	-7.3480	0.0433	8.1759
CIA	-4.2623	-3.0375	0.0000	5.2339
PANI-CIA	-3.1112	-10.8808	2.0278	11.4971

Table 4 : TDDFT

PANI-3HBZA			
Wave Length (nm)	**Oscillatory Strength**	**Orbital**	**% Contribution**
366.9	0.7614	88a → 94a 89a → 94a	47.98 29.07
PANI-CIA			
440.8	0.2818	95a → 97a	78.33
312.8	0.1682	86a → 97a 88a → 97a	35.87 32.70

Table 5: Frontier Molecular Orbital

	CIA	3HBZA	PANI-CIA	PANI-3HBZA
Band Gap (eV)	4.9	5.1	3.0	2.1
Ionisation Potential (eV)	6.7	6.3	6.3	6.1
Electron Affinity (eV)	1.8	1.1	3.3	4.0
Electronic chemical Potential (eV)	-4.2	-3.7	-4.8	-5.1
Chemical Hardness (eV)	2.5	2.6	1.5	1.1
Global Softness (eV)	0.4	0.4	0.7	0.9
Electrophilic index (eV)	22.2	17.7	17.5	13.7
Absolute Electro negativity (eV)	4.2	3.7	4.8	5.1
$\mathbf{Q^{Max}}$	1.7	1.4	3.2	4.8

Table 6: Polarisability (Au)

Axis	**3HBZA**	**CIA**	**PANI-3HBZA**	**PANI-CIA**
μ_Z	3.02×10^{-15}	3.86×10^{-15}	1.70×10^{-02}	0.798
α_{XZ}	1.34×10^{-10}	9.46×10^{-11}	14.9	22.8
α_{YZ}	9.83×10^{-11}	-4.20×10^{-11}	7.30	16.8
α_{ZZ}	29.9	34.9	99.3	164
β_{XZZ}	1.54	0.389	23.1	-362
β_{YZZ}	0.347	0.987	18.3	-126
β_{ZZZ}	-6.16×10^{-10}	-2.39×10^{-09}	-2.59	-166
γ_{ZZZZ}	55.5	60.0	849	8930

Table 7 : Conductance

PANI-3HBZA

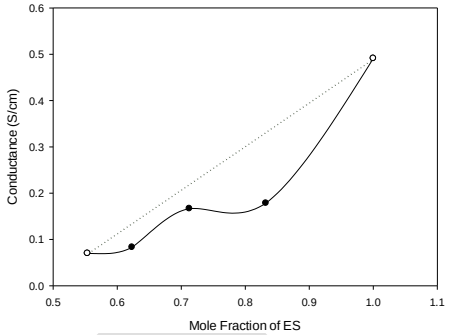

Mole Fraction of PANI	Conductance S/cm
1.0000	0.4910
0.8322	0.1783
0.7126	0.1665
0.6231	0.0830
0.5535	0.0698

	R	y_0	a	b
Ideal	1.0	-0.4524	0.9434	-
Real	0.9804	0.8493	-2.6461	2.2761

PANI-CIA

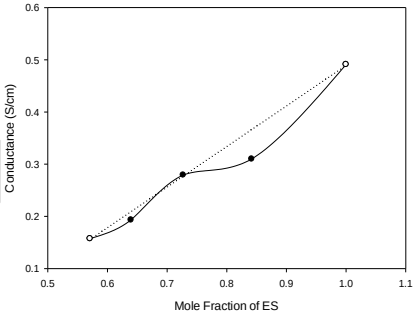

Mole Fraction of PANI	Conductance S/cm
1	0.491
0.8418	0.3098
0.7268	0.2792
0.6394	0.1931
0.5708	0.1572

	R	y_0	a	b
Ideal	1.0	-0.4524	0.9434	-
Real	0.9879	0.1249	-0.3241	0.6834